

# Understanding the effect of marginal exciton – charge-transfer state offsets on charge generation and recombination in polymer:fullerene solar cells

Michelle S. Vezie<sup>1#</sup>, Mohammed Azzouzi<sup>1#</sup>, Andrew M. Telford<sup>1</sup>, Tom Hopper<sup>2</sup>, Alex Sieval<sup>6</sup>, J. C. Hummelen<sup>6</sup>, Hugo Bronstein<sup>5,7</sup>, Thomas Kirchartz<sup>3,4</sup>, Artem Bakulin<sup>2</sup>, Tracey M. Clarke<sup>5</sup> and Jenny Nelson<sup>1,\*</sup>

<sup>1</sup> Department of Physics and Centre for Plastic Electronics, Imperial College London, London SW7 2AZ, United Kingdom.

<sup>2</sup> Department of Chemistry and Centre for Plastic Electronics, Imperial College London, London SW7 2AZ, United Kingdom

<sup>3</sup> IEK5-Photovoltaics, Forschungszentrum Jülich, 52425 Jülich, Germany

<sup>4</sup> Faculty of Engineering and CENIDE, University of Duisburg-Essen, Carl-Benz-Str. 199, 47057 Duisburg, Germany

<sup>5</sup> Department of Chemistry, University College London, Christopher Ingold Building, London WC1H 0AJ, United Kingdom

<sup>6</sup> Solenne

<sup>7</sup> Department of Chemistry, University of Cambridge, Lensfield Road, Cambridge, CB2 1EW

\* Corresponding Author: [jenny.nelson@imperial.ac.uk](mailto:jenny.nelson@imperial.ac.uk)

[# These authors contributed equally](#)

## ABSTRACT

The energetic offset between the photoexcited state and charge-transfer (CT) state in organic heterojunction solar cells influences both charge generation and open circuit voltage ( $V_{oc}$ ). In this work, we use time resolved spectroscopy and voltage loss measurements to analyse the charge generation and recombination processes in blends of a low-bandgap isoindigoid polymer with fullerenes of different electron affinity. The system allows us to compare the effect of exciton-CT state offset on charge separation and recombination in chemically similar systems and on charge (electron or hole) transfer within the same system. In the case of the lowest exciton-CT state offset, charge recombination dynamics are distinctly faster than in other cases and photocurrent generation is lower but significant. The faster recombination is surprising given that the higher LUMO fullerene blends shows higher  $V_{oc}$  and lower non-radiative voltage losses. We show that the observations are reconciled using a model for the dependence of  $V_{oc}$  on radiative and non-radiative recombination. We also explain the effect of exciting donor or acceptor on charge transfer and recombination using a simple kinetic model. The results of the model show that hybridisation between lowest excitonic and CT states significantly can reduce  $V_{oc}$  losses whilst still allowing reasonable charge generation efficiency.

## INTRODUCTION

In organic solar cells, the heterojunction between electron donor and electron acceptor provides the driving energy for charge separation, as well as the interface at which recombination occurs [1]. In the common picture of device function, both charge separation and charge recombination proceed via a manifold of excitonic and charge-transfer (CT) excited states that extend locally over the donor and/or acceptor medium [2–6]. The driving energy can be quantified as the energetic offset between the local photoexcited exciton (donor or acceptor) and the lowest energy charge-transfer state. Whilst some reports have indicated that charge generation efficiency decreases when this offset is decreased [7–9], others report efficient pair generation at negligible apparent offset in polymer:fullerene [10] and increasingly in polymer:non-fullerene acceptor [11] blends. The effect of excitation energy on charge pair generation has also been controversial [12–14].

Whilst a large offset may benefit photocurrent, smaller offsets benefit open-circuit voltage  $V_{oc}$ . Organic solar cells show relatively small  $qV_{oc}$  (where  $q$  is electronic charge) relative to optical gap, compared to values in good inorganic solar cells [15].  $qV_{oc}$  is empirically linked to the energy of the lowest CT state,  $E_{CT}$  [16]; the low  $V_{oc}$  can be assigned partly to the effect of the heterojunction in reducing the generated electrochemical potential relative to that which could, theoretically, be generated in either donor or acceptor material alone. Low  $V_{oc}$  also results from the relatively high rate of non-radiative recombination that is observed in organic heterojunction solar cells [17,18]. The loss in  $V_{oc}$  due to non-radiative recombination can be quantified as

$\Delta V_{oc,nr} = \frac{kT}{q} \ln\left(\frac{1}{QE_{EL}}\right)$  where  $QE_{EL}$  is the radiative quantum efficiency of the device.

While the best silicon solar cell has  $\Delta V_{oc,nr} < 0.15 \text{ V}$  ( $QE_{EL} < 3 \cdot 10^{-3}$ ), organic donor:acceptor heterojunction solar cells have  $\Delta V_{oc,nr}$  in the range 0.20 – 0.55 V with

$QE_{EL}$  usually well below  $10^{-5}$  [11,15,19,20]. Whilst  $V_{oc}$  could be raised by reducing the energetic offset, low offset reduces the driving force for charge separation and may reduce charge separation efficiency or enhance geminate recombination. A relevant question, therefore, is how far  $V_{oc}$  can be raised by reducing the energetic offset at the heterojunction: *in particular, how does a small offset influence recombination kinetics?* To understand the mechanism of interfacial charge transfer processes a further question is how the choice of photo-excited component (donor or acceptor) influences the charge transfer efficiency and recombination kinetics, given that the donor and acceptor exciton, in general, present different offsets relative to the CT state.

In this work we study a low bandgap polymer combined with two different fullerene derivatives, one of which provides a large, and the other a small, interfacial energy offset for electron transfer, while both provide large offsets for hole transfer. We use ultrafast transient absorption and pump-push-photocurrent spectroscopy to show that, upon excitation of the donor, the lower-offset blend exhibits shorter charge lifetimes, despite showing the larger open-circuit voltage and a lower non-radiative voltage loss. With the aid of a model of non-radiative recombination via the charge-transfer state and a kinetic model we can explain the behaviour in terms of the impact of CT and singlet state mixing on the oscillator strength of the CT state. The results suggests a useful design rule for high-voltage organic solar cell materials.

## RESULTS

### Material system and device performance

We study the low band gap isoindigoid based polymer indolo-naphthyridine-6,13-dione thiophene-co-selenophene (INDT-S) [21] combined with two fullerene

derivatives of different electron affinity, the widely studied phenyl  $C_{61}$  butyric methyl acid ester (PCBM) and a new ketolactam fullerene derivative KLOC-6 (KL) (see SI section S1 for details of synthesis) (Figure 1((a)). The INDT-S:PCBM system presents a nominal LUMO(Donor) – LUMO(Acceptor) difference of -0.02 eV, taking the INDT-S LUMO as -3.77 eV (from a photoelectron spectroscopy estimate of the HOMO energy plus the optical gap [22]) and the PCBM LUMO as -3.75 eV (from cyclic voltammetry [table S1, fig S1]). The LUMO of KL lies 170 meV deeper than PCBM, also determined by CV, leading to a LUMO difference of around 0.15 eV for the INDT-S:KL blend. The HOMO energy differences are large ( $> 0.5$  eV) in both blends. Although the estimates of the offset energies in blend films are uncertain [21] (due to differences in measurement, and uncertainties in translating MO energy differences into state energy offsets) the two combinations represent a high-offset and low-offset donor:acceptor blend for electron transfer. Since both fullerenes are  $C_{60}$  derivatives their optical absorption properties are almost identical leading to very similar absorption profiles for the blend films (SI Fig S2). For both blends the donor absorption (maximum during 600 – 900 nm) is spectrally separated from the acceptor absorption ( $< 500$  nm), allowing the donor and acceptor component to be selectively excited: excitation by red light can only stimulate electron transfer while excitation by blue light primarily stimulates hole transfer.

Current density-voltage and internal quantum efficiency (IQE, defined as the current collected per photon absorbed) data are displayed in Figure 1(b,c). Sample and device preparation details are given in the Methods section of the SI. The data clearly show that more current is generated, per absorbed photon, from excitation of the polymer in the KL blend than in the PC<sub>61</sub>BM blend, resulting in greater overall short circuit current density. Furthermore, there is no evidence of wavelength-dependent

photogeneration efficiency within the region where only the polymer absorbs, in contrast to some previous reports [4]. At shorter wavelengths the data are more susceptible to interference effects, [23] and so no reliable comparisons can be made of the two spectra in the region where the acceptor absorbs (< 500 nm). The IQE was calculated using the external quantum efficiency (EQE) in conjunction with experimental reflectivity measurements and parasitic absorption simulated using measured complex refractive index data for the materials and an optical model [24]; see SI Section S3 for full details. Whilst the efficiency of current generation from the polymer is higher in the high-offset KL blend than in the low-offset PCBM blend, the latter is clearly not negligible. For comparison, the external quantum efficiency of a pristine INDT-S device is no greater than 0.05% suggesting an IQE of much less than 0.5% (Figure S4).

Figure 1(c) shows that the  $V_{oc}$  of the KL blend under AM 1.5 illumination is smaller than that of the PCBM blend, as would be expected from its smaller difference in LUMO energies. To quantify the voltage difference we measure electroluminescence and high-dynamic-range external quantum efficiency (EQE) spectra of both blends (Figure 1d and Figures S5(a) and S5(b)), and extract the open-circuit voltage in the radiative limit,  $V_{oc,rad}$ , and the non-radiative voltage loss  $\Delta V_{oc,nr} = V_{oc,rad} - V_{oc}$  (Table 1, see Ref. [15] for details of the method.) The calculated  $V_{oc,rad}$  is almost identical for the two blends despite the significant difference in energy level offsets, while  $\Delta V_{oc,nr}$  is larger by 0.1V for the INDTS:KL device ( $\Delta V_{oc,nr} = 0.48$  V) than the INDTS:PCBM device ( $\Delta V_{oc,nr} = 0.35$  V), and  $QE_{EL}$  correspondingly smaller. Consistent with the improved  $QE_{EL}$  of the PCBM device, its electroluminescence intensity is much higher than that of the KL device under similar injection current.

## Spectroscopy measurements

To better understand the kinetics of the excited species we study films of both blends using transient absorption spectroscopy (TAS) and Pump-push-probe (PPP) measurement. Microsecond TAS yields the spectra of long lived species, in all cases consisting of a broad feature centred around 1600 nm assigned to the polymer cation and a band at 1100-1300 nm assigned to the fullerene anion (SI Figure S6). Triplets can be ruled out by the insensitivity of the kinetics to oxygen (SI Fig S7). By comparing the absorption at 1600nm 400ns after polymer excitation (figure S6), it is clear that long-lived charge generation following polymer excitation is approximately twice as efficient in the high-offset KL blend as in the low-offset PCBM blend. For each blend the TAS spectra are similar for excitation of polymer and fullerene, suggesting the same long-lived species are generated on the microsecond time scale irrespective of which component is photoexcited.

We then apply picosecond transient absorption spectroscopy (ps-TAS) to both blend films to probe the photo-excited states on short time scales exciting either the polymer alone (800 nm pump), or predominantly the fullerene by pumping at the wavelength where polymer absorption is minimized (450 nm). All spectra show a broad transient band peaking above 1300 nm which reflects exciton absorption (SI Fig S8 for full ps-TAS spectra). At ns times the spectra of both blends show features that resemble the microsecond spectra and indicate charge generation via the bands at 1000 – 1300 nm that are assigned to the fullerene anion [25]. To study charge dynamics, the probe wavelength of 1200 nm was chosen to capture absorption by charged species but will inevitably also contain some polymer singlet absorption (SI Table S9).

Fig 2 shows the ps-TAS kinetics of the blends when excited at 800 nm or 450 nm and probed at 1200 nm. When pumped at 800 nm (Figure 2a), the INDT-S:PCBM blend shows a fast, approximately exponential, decay with  $\sim 20$  ps lifetime while the INDT-S:KL blend decays much more slowly with almost 25 % of the initial signal amplitude still present after 6 ns. Somewhat surprisingly, the ps-TAS kinetics of the pristine polymer pumped at 800 nm are almost identical to those of the PCBM blend, showing exponential kinetics with a ca 20 ps lifetime, consistent with a previous report for the polymer  $S_1$  state lifetime (23 ps) [22], even though only the INDT-S:PCBM blend spectrum shows evidence of charge generation. Assuming that the assignment of the 1050–1250 nm feature to fullerene anions is correct, the kinetics would suggest that INDT-S:PCBM undergoes both ultrafast charge generation and very rapid geminate recombination. The short lifetime of the charges visible in the PCBM blend spectra is consistent with the charge pair states in this low-offset system being tightly bound [26].

In contrast, pumping the blends at 450 nm leads to slow, multiphasic TAS decays for both blends (Figure 2b), similar in kinetics to the KL blend when pumped at 800 nm, as well as evidence for fullerene anion generation (Fig S8). At this wavelength, primarily the fullerene is excited so hole, rather than electron, transfer would follow. Note that both blends are high-offset for hole transfer. The ps-TAS data thus provide evidence for long-lived charges in all cases where there is a high exciton-CT state offset driving charge separation, but rapid excited-state (exciton and charge pair) decay, occurring on a similar time scale to polymer exciton decay, when the offset is different nature dominate the TAS decay compared to the high-offset cases.

In order to probe the nature of the photo-excited species in the blends at ps timescales, we performed optical control visible-pump/IR-push spectroscopy with

photocurrent detection (PPP) [6,27]. The devices were measured under identical conditions and photocurrent normalized to the reference photocurrent, therefore the absolute values of the response can be directly compared and reflect the fraction of bound charge pairs in the systems. The greatest number of bound charges at early times is observed under 800 nm excitation, when only electron transfer is possible (SI Fig S10(a)). At this wavelength, the photocurrent pulse amplitude in the PCBM blend is one order of magnitude larger than in the KL blend, indicating that the number of bound charges has increased 10-fold and the efficiency of charge separation has therefore reduced, consistent with the reduced offset driving charge separation.

At 400 nm excitation, where hole transfer dominates the photophysics of both materials and the offset driving charge transfer is greater, we observe a much lower number of bound charge pairs in both cases. However, the KL blend still exhibits fewer bound charges than the PCBM blend.

The kinetics of the PPP and ps-TAS data for 800 nm excitation for the different blends as well as the pristine INDT-S can be compared by normalizing the two signals, see Figure 3. It is clear from these data that the decays of the PPP and ps-TAS signals following polymer excitation for the INDT-S:PC<sub>61</sub>BM case are very similar. However, for the INDT-S:KL case, the kinetics of the two experiments are very different. TAS gives a measure of all charges, while PPP is only sensitive to bound charges. Therefore this comparison clearly shows that for 800 nm excitation in the INDT-S:KL blend, significant numbers of unbound charges are being generated, showing a different, slower decay kinetics than the bound fraction of photo-generated charges that are monitored by PPP. Meanwhile, for 800 nm excitation in the PC<sub>61</sub>BM blend and in the pure polymer, the decay is dominated by bound charge

pairs that are generated quickly but recombine rapidly in the absence of the push pulse. For the 400nm excitation, the decay of the photo-excited charges for the two blends probed using TAS and the PPP experiment are similar to the case of the INDT-S:KL blend probed at 800nm i.e: showing a slow shoulder in the TAS signal confirming the generation of a significant number of unbound charges (Figure S10(b)).

## Time-dependent density functional calculations of the excited states

To characterise the interfacial states we calculate the excited states for the donor (modelled as a dimer of INDT-S), the fullerene acceptor and the donor: acceptor pair, for each fullerene type, and analyse the nature of the excited states using density functional theory (DFT) (B3LYP/6-31G\*) and time dependent-DFT (TDDFT), see SI Section S11 for details [28]. Although the two-molecule system is a crude model of a blend film that supports many more excited states [29,30] and CT character is generally not well modelled by TDDFT, these calculations serve as a guide to the nature of the lowest excited states. Calculations for donor and acceptor alone support the smaller LUMO-LUMO difference for INDT-S:PCBM than INDT-S:KL. For the two donor: acceptor pairs, the first singlet excited state lies at similar energy, but the INDT-S:KL state has strong charge-transfer character (0.75 electron transferred) and a low oscillator strength for the transition to ground state while the lowest INDT-S:PCBM excited state has weak charge-transfer character (0.1 e transferred) and an oscillator strength an order of magnitude higher. The mixed excitonic-CT nature of the lowest INDT-S:PCBM state suggests hybridisation of the donor exciton and the CT state, consistent with the intensity borrowing effect [31]. The trend in oscillator strength is consistent with electroluminescence data which indicate, from the similar positions of electroluminescence peaks for pristine and blend films, that polymer and

CT state emission are mixed, and show much brighter electroluminescence from the PCBM than KL blends (see SI fig S5(a)).

## DISCUSSION / CONCLUSION :

We now endeavour to explain the different charge generation and recombination behaviour of the two blend systems. To summarise the observations, both blend devices showed efficient charge generation as compared to the pristine donor device, when either donor or acceptor is excited, but charge generation following polymer excitation is twice as efficient for the KL than the PCBM blend. The evolution of the excited states as inferred from TAS and PPP measurement appeared to be mostly affected by the difference in energy between the photogenerated exciton and the CT state: 1) when the difference is significant (exciting the acceptor in either case and exciting the donor in the KL case) photoexcited species decay slowly on a several ns time scale, and the slow kinetics are assigned to species that are unaffected by the push laser in the PPP experiment. 2) When the difference is small (exciting the donor in the PCBM:INDT-S) the evolution of the excited states is similar to the pristine polymer case both in the TAS and the PPP measurement; similar kinetics for TAS and PPP suggest photogenerated charge pairs are bound. Moreover the calculated excited states for blends using TDDFT, suggest that the lowest excited state for the PCBM:INDT-S blend possesses a more excitonic behaviour (lower degree of charge transfer and higher oscillator strength) than in the KL:INDT-S case.

First, to explain the different kinetics observed in the different cases, we propose a kinetic model where the exciton transfers to a CT state with a rate  $K_{trans}^e$  or  $K_{trans}^h$  corresponding to the rate of electron transfer or hole transfer respectively,

subsequently the charge transfer state formed can either recombine with a rate  $K_{rec}^{CT}$  or form a charge-separated state with a rate  $K_{trans}^{CT,CS}$  (Figure 4a, the model equations are presented in Section S12 of the SI). By fitting the ps-TAS signals using the model and experimentally determined parameters we estimated the rate constant for each of the processes described (Table 2). These results show that the surprising similarity between the excited state evolution for the pristine donor and the PCBM:INDT-S when excited with a 800nm laser pulse can be explained by the slow electron transfer ( $K_{trans}^e \sim 0.015 \text{ ps}^{-1}$ ) due to the low energy difference between the exciton state and the CT state. A faster rate of hole transfer rate of  $K_{trans}^h \sim 0.3 \text{ ps}^{-1}$  reproduces the decay of the excited charges when exciting the acceptor (400nm) (figure S12(b)). This difference in the net rates is expected from the energy difference of the two states, the large energy offset would increase the rate of charge transfer [32]. This enforces the fact that the difference between the photo-generation process when the donor is photo-excited and when the acceptor is photo-excited can be explained by a difference between the rate of charge transfer from the exciton state to the CT state, without changing any other parameter. Interestingly, when considering perfect collection from the charge-separated state (back transfer to the CT state and their recombination is neglected), and using the rates in table 1, a percentage of generated charges similar to the IQE values at 800nm is predicted (10% for the PCBM:INDT-S and around 33% for the KL:INDT-S blend) (figure S12(c)).

To explain the difference in the  $V_{oc}$  of the two devices we consider the effect of interfacial CT state properties on recombination using a model we recently developed [33]. From the voltage loss analysis, we have established that the difference in the voltage of the two devices was related to the difference in their

non-radiative losses (0.35 V for the PCBM devices and 0.48 for the KL devices). The properties of the interfacial CT state can be directly related to  $\Delta V_{oc, nr}$  [33,34]. Since we know that the CT state of INDT-S:PCBM differs from that of INDT-S:KL by having higher energy and oscillator strength (from the TDDFT calculation and the electroluminescence measurement), we implement the differences in these two properties into the model (SI section S13) [33]. We find that the 100 meV increase in  $E_{CT}$  from INDT-S:KL to INDT-S:PCBM first increases  $V_{oc}$  by 40 mV, whereas an increase of the CT-state oscillator strength by two orders-of-magnitude increases  $V_{oc}$  by an additional 60 mV, such that their combined effect can explain the change in the  $V_{oc}$  between these two devices (figure 4, Table S3). The simultaneous increase of the CT state energy and its oscillator strength can be explained by the hybridisation of the two states due to the small energy difference between the LUMO levels of the PCBM:INDT-S blend [35]. Moreover, the model results show that the total rate of CT state recombination is increased in the PCBM blend relative to the KL case, despite the increased  $V_{oc}$ . Although the magnitudes of the recombination rate obtained from the voltage losses model are larger than the experimental ones, the trend in the CT state recombination rate agrees with the results of the fits presented in table 2. The discrepancy in rates indicates that the model relating recombination to  $V_{oc}$  is not sufficiently complex to describe experimental systems quantitatively, for example through neglect of disorder [36].

In conclusion, in this work we have studied the effect of the energy offset on the charge carrier dynamics, photocurrent generation and  $V_{oc}$  in polymer: fullerene solar cells. We have found that despite the insignificant energy offset for electron transfer in the PCBM:INDT-S blend, the charge generation process was significantly more efficient than the pristine INDT-S devices. From the picosecond dynamics of

the photo-excited states, we have established that the low energy offset results in a lower electron transfer rate from the exciton to the CT state without further affecting the other charge generation processes (compared to case where the acceptor was photo-excited). On the other hand the increased  $V_{oc}$  for the low energy offset blend was explained by a coupled effect: an increase in the CT state energy, and the increase of the CT state to ground state transition's oscillator strength. The increased oscillator strength for the low offset cases is likely to result from mixing of the exciton and CT states and the associated intensity borrowing mechanism. The study suggests that by careful tuning of the exciton to CT-state offset and consideration of electron and hole transfer contributions, high  $V_{oc}$  values may be achieved whilst maintaining useful photocurrents.

## REFERENCES

- [1] S. R. Cowan, N. Banerji, W. L. Leong, and A. J. Heeger, *Charge formation, recombination, and sweep-out dynamics in organic solar cells*, *Adv. Funct. Mater.* **22**, 1116 (2012).
- [2] J.-L. Brédas, J. E. Norton, J. Cornil, and V. Coropceanu, *Molecular Understanding of Organic Solar Cells: The Challenges*, *Acc. Chem. Res.* **42**, 1691 (2009).
- [3] T. M. Clarke and J. R. Durrant, *Charge Photogeneration in Organic Solar Cells*, *Chem. Rev.* **110**, 6736 (2010).
- [4] S. D. Dimitrov, A. A. Bakulin, C. B. Nielsen, B. C. Schroeder, J. Du, H. Bronstein, I. McCulloch, R. H. Friend, and J. R. Durrant, *On the energetic dependence of charge separation in low-band-gap polymer/fullerene blends*, *J. Am. Chem. Soc.* **134**, 18189 (2012).
- [5] S. D. Dimitrov, C. B. Nielsen, S. Shoaee, P. Shakya Tuladhar, J. Du, I. McCulloch, and J. R. Durrant, *Efficient charge photogeneration by the dissociation of PC 70BM excitons in polymer/fullerene solar cells*, *J. Phys. Chem. Lett.* **3**, 140 (2012).
- [6] A. A. Bakulin, S. D. Dimitrov, A. Rao, P. C. Y. Chow, C. B. Nielsen, B. C. Schroeder, I. McCulloch, H. J. Bakker, J. R. Durrant, and R. H. Friend, *Charge-transfer state dynamics following hole and electron transfer in organic photovoltaic devices*, *J. Phys. Chem. Lett.* **4**, 209 (2013).
- [7] H. Ohkita, S. Cook, Y. Astuti, W. Duffy, S. Tierney, W. Zhang, M. Heeney, I. McCulloch, J. Nelson, D. D. C. Bradley, and J. R. Durrant, *Charge Carrier Formation in Polythiophene/Fullerene Blend Films Studied by Transient Absorption Spectroscopy*, *J. Am. Chem. Soc.* **130**, 3030 (2008).
- [8] B. P. Rand, D. P. Burk, and S. R. Forrest, *Offset energies at organic semiconductor heterojunctions and their influence on the open-circuit voltage of thin-film solar cells*, *Phys. Rev. B* **75**, 115327 (2007).
- [9] M. A. Faist, T. Kirchartz, W. Gong, R. S. Ashraf, I. McCulloch, J. C. De Mello, N. J. Ekins-Daukes, D. D. C. Bradley, and J. Nelson, *Competition between the charge transfer state and the singlet states of donor or acceptor limiting the efficiency in polymer: Fullerene solar cells*, *J. Am. Chem. Soc.* **134**, 685 (2012).
- [10] K. Vandewal, Z. Ma, J. Bergqvist, Z. Tang, E. Wang, P. Henriksson, K. Tvingstedt, M. R. Andersson, F. Zhang, and O. Inganäs, *Quantification of Quantum Efficiency and Energy Losses in Low Bandgap Polymer:Fullerene Solar Cells with High Open-Circuit Voltage*, *Adv. Funct. Mater.* **22**, 3480 (2012).
- [11] D. Qian, Z. Zheng, H. Yao, W. Tress, T. R. Hopper, S. Chen, S. Li, J. Liu, S. Chen, J. Zhang, X.-K. Liu, B. Gao, L. Ouyang, Y. Jin, G. Pozina, I. A. Buyanova, W. M. Chen, O. Inganäs, V. Coropceanu, J.-L. Bredas, H. Yan, J. Hou, F. Zhang, A. A. Bakulin, and F. Gao, *Design rules for minimizing voltage losses in high-efficiency organic solar cells*, *Nat. Mater.* **17**, 703 (2018).

- [12] S. Albrecht, K. Vandewal, J. R. Tumbleston, F. S. U. Fischer, J. D. Douglas, J. M. J. Fréchet, S. Ludwigs, H. Ade, A. Salleo, and D. Neher, *On the Efficiency of Charge Transfer State Splitting in Polymer:Fullerene Solar Cells*, *Adv. Mater.* **26**, 2533 (2014).
- [13] K. Vandewal, S. Albrecht, E. T. Hoke, K. R. Graham, J. Widmer, J. D. Douglas, M. Schubert, W. R. Mateker, J. T. Bloking, G. F. Burkhard, A. Sellinger, J. M. J. Fréchet, A. Amassian, M. K. Riede, M. D. McGehee, D. Neher, and A. Salleo, *Efficient charge generation by relaxed charge-transfer states at organic interfaces*, *Nat. Mater.* **13**, 63 (2013).
- [14] C. Silva, *Some like it hot*, *Nat. Mater.* **12**, 5 (2013).
- [15] J. Yao, T. Kirchartz, M. S. Vezie, M. A. Faist, W. Gong, Z. He, H. Wu, J. Troughton, T. Watson, D. Bryant, and J. Nelson, *Quantifying Losses in Open-Circuit Voltage in Solution-Processable Solar Cells*, *Phys. Rev. Appl.* **4**, 014020 (2015).
- [16] K. Vandewal, K. Tvingstedt, A. Gadisa, O. Inganäs, and J. V. Manca, *On the origin of the open-circuit voltage of polymer–fullerene solar cells*, *Nat. Mater.* **8**, 904 (2009).
- [17] R. A. J. Janssen and J. Nelson, *Factors limiting device efficiency in organic photovoltaics*, *Adv. Mater.* **25**, 1847 (2013).
- [18] M. Azzouzi, T. Kirchartz, and J. Nelson, *Factors Controlling Open-Circuit Voltage Losses in Organic Solar Cells*, *Trends Chem.* **1**, 49 (2019).
- [19] D. Baran, R. S. Ashraf, D. A. Hanifi, M. Abdelsamie, N. Gasparini, J. A. Röhr, S. Holliday, A. Wadsworth, S. Lockett, M. Neophytou, C. J. M. Emmott, J. Nelson, C. J. Brabec, A. Amassian, A. Salleo, T. Kirchartz, J. R. Durrant, and I. McCulloch, *Reducing the efficiency–stability–cost gap of organic photovoltaics with highly efficient and stable small molecule acceptor ternary solar cells*, *Nat. Mater.* **16**, 363 (2017).
- [20] M. E. Ziffer, S. Byeok Jo, H. Zhong, L. Ye, H. Liu, F. Lin, J. Zhang, X. Li, H. W. Ade, A. K-Y Jen, D. S. Ginger, H. Kong, S. B. Jo, H. Zhong, L. Ye, H. Liu, F. Lin, J. Zhang, X. Li, H. W. Ade, A. K.-Y. Jen, D. S. Ginger, S. Byeok Jo, H. Zhong, L. Ye, H. Liu, F. Lin, J. Zhang, X. Li, H. W. Ade, A. K-Y Jen, and D. S. Ginger, *Long-Lived, Non-Geminate, Radiative Recombination of Photogenerated Charges in a Polymer/Small-Molecule Acceptor Photovoltaic Blend*, *J. Am. Chem. Soc.* **140**, 9996 (2018).
- [21] J. Sworakowski, J. Lipiński, and K. Janus, *On the reliability of determination of energies of HOMO and LUMO levels in organic semiconductors from electrochemical measurements. A simple picture based on the electrostatic model*, *Org. Electron.* **33**, 300 (2016).
- [22] K. J. Fallon, N. Wijeyasinghe, E. F. Manley, S. D. Dimitrov, S. A. Yousaf, R. S. Ashraf, W. Duffy, A. A. Y. Guilbert, D. M. E. Freeman, M. Al-Hashimi, J. Nelson, J. R. Durrant, L. X. Chen, I. McCulloch, T. J. Marks, T. M. Clarke, T. D. Anthopoulos, and H. Bronstein, *Indolo-naphthyridine-6,13-dione Thiophene Building Block for Conjugated Polymer Electronics: Molecular Origin of Ultrahigh n-Type Mobility*, *Chem. Mater.* **28**, 8366 (2016).

- [23] K. O. Sylvester-Hvid, T. Ziegler, M. K. Riede, N. Keegan, M. Niggemann, and A. Gombert, *Analyzing poly(3-hexyl-thiophene):1-(3-methoxy-carbonyl)propyl-1-phenyl-(6,6)C61 bulk-heterojunction solar cells by UV-visible spectroscopy and optical simulations*, J. Appl. Phys. **102**, 054502 (2007).
- [24] G. F. Burkhard, E. T. Hoke, and M. D. McGehee, *Accounting for Interference, Scattering, and Electrode Absorption to Make Accurate Internal Quantum Efficiency Measurements in Organic and Other Thin Solar Cells*, Adv. Mater. **22**, 3293 (2010).
- [25] S. Yamamoto, J. Guo, H. Ohkita, and S. Ito, *Formation of Methanofullerene Cation in Bulk Heterojunction Polymer Solar Cells Studied by Transient Absorption Spectroscopy*, Adv. Funct. Mater. **18**, 2555 (2008).
- [26] S. D. Dimitrov, M. Azzouzi, J. Wu, J. Yao, Y. Dong, P. S. Tuladhar, B. C. Schroeder, E. R. Bittner, I. McCulloch, J. Nelson, and J. R. Durrant, *Spectroscopic Investigation of the Effect of Microstructure and Energetic Offset on the Nature of Interfacial Charge Transfer States in Polymer: Fullerene Blends*, J. Am. Chem. Soc. **141**, 4634 (2019).
- [27] A. A. Bakulin, A. Rao, V. G. Pavelyev, P. H. M. van Loosdrecht, M. S. Pshenichnikov, D. Niedzialek, J. Cornil, D. Beljonne, and R. H. Friend, *The role of driving energy and delocalized states for charge separation in organic semiconductors*, Science (80-. ). **335**, 1340 LP (2012).
- [28] S. Few, J. M. Frost, J. Kirkpatrick, and J. Nelson, *Influence of Chemical Structure on the Charge Transfer State Spectrum of a Polymer:Fullerene Complex*, J. Phys. Chem. C **118**, 8253 (2014).
- [29] E. R. Bittner and C. Silva, *Noise-induced quantum coherence drives photo-carrier generation dynamics at polymeric semiconductor heterojunctions.*, Nat. Commun. **5**, 3119 (2014).
- [30] G. Raos, M. Casalegno, and J. Idé, *An Effective Two-Orbital Quantum Chemical Model for Organic Photovoltaic Materials*, J. Chem. Theory Comput. **10**, 364 (2014).
- [31] M. Bixon, J. Jortner, J. Cortes, H. Heitele, and M. E. Michel-Beyerle, *Energy Gap Law for Nonradiative and Radiative Charge Transfer in Isolated and in Solvated Supermolecules*, J. Phys. Chem. **98**, 7289 (1994).
- [32] C. L. Braun, *Electric field assisted dissociation of charge transfer states as a mechanism of photocarrier production*, J. Chem. Phys. **80**, 4157 (1984).
- [33] M. Azzouzi, J. Yan, T. Kirchartz, K. Liu, J. Wang, H. Wu, and J. Nelson, *Nonradiative Energy Losses in Bulk-Heterojunction Organic Photovoltaics*, Phys. Rev. X **8**, 031055 (2018).
- [34] J. Benduhn, K. Tvingstedt, F. Piersimoni, S. Ullbrich, Y. Fan, M. Tropiano, K. A. McGarry, O. Zeika, M. K. Riede, C. J. Douglas, S. Barlow, S. R. Marder, D. Neher, D. Spoltore, and K. Vandewal, *Intrinsic non-radiative voltage losses in fullerene-based organic solar cells*, Nat. Energy **2**, 17053 (2017).
- [35] F. D. Eisner, M. Azzouzi, Z. Fei, X. Hou, T. D. Anthopoulos, T. J. S. Dennis, M. Heeney, and J. Nelson, *Hybridization of Local Exciton and Charge-Transfer States Reduces Nonradiative Voltage Losses in Organic Solar Cells*, J. Am.

Chem. Soc. jacs. 9b01465 (2019).

- [36] G. D. ' Avino, L. Muccioli, Y. Olivier, and D. Beljonne, *Charge Separation and Recombination at Polymer–Fullerene Heterojunctions: Delocalization and Hybridization Effects*, *J. Phys. Chem. Lett* **7**, 12 (2016).

FIGURES:

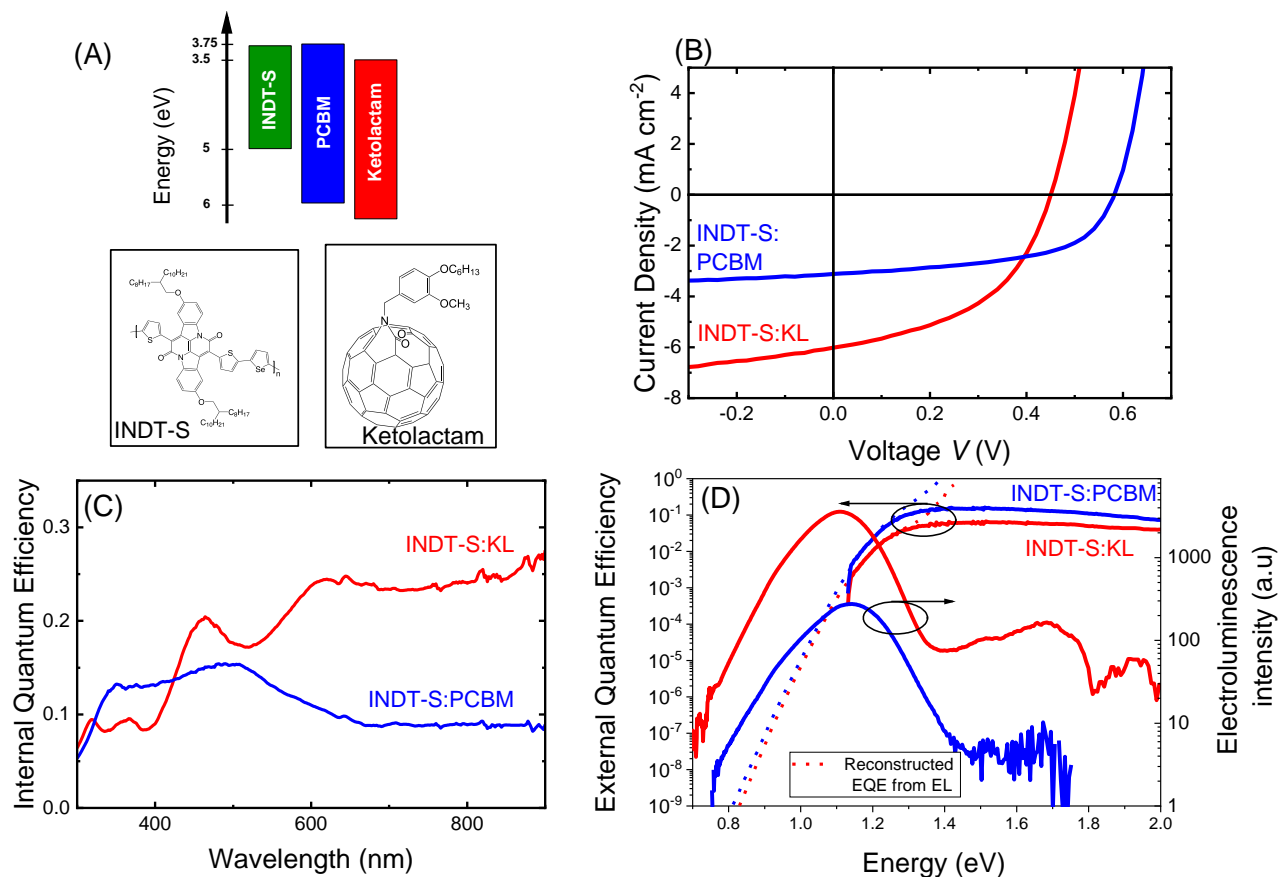


Figure 1 : (a) Chemical structures of IND-T-S and Ketolactam, with the HOMO and LUMO levels as calculated using either CV or photoelectron spectroscopy. (b) J-V characteristics of the two blends IND-T-S:PCBM and IND-T-S:KL and (c) IQE of the two devices as calculated using the method presented in the SI. (d) EQE and Electroluminescence of the two devices, with the extended EQE using the reciprocity between EL and EQE. The EL spectra is taken for an injection current of 20mAcm<sup>-2</sup>

**Table 1: Solar cell parameters extracted from current voltage curves and from the luminescence based voltage loss analysis for the two blends.**

<b>Blend</b>	<b><math>J_{sc}</math> [mA/cm<sup>2</sup>]</b>	<b>PCE</b>	<b>FF</b>	<b><math>V_{oc}</math> [V]</b>	<b><math>V_{oc,rad}</math> [V]</b>	<b><math>\Delta V_{oc,nr}</math> [V]</b>
INDT-S:Ketolactam	6.02	1.28%	0.46	0.46	0.94	0.48
INDT-S:PCBM	3.12	1.01%	0.56	0.58	0.93	0.35

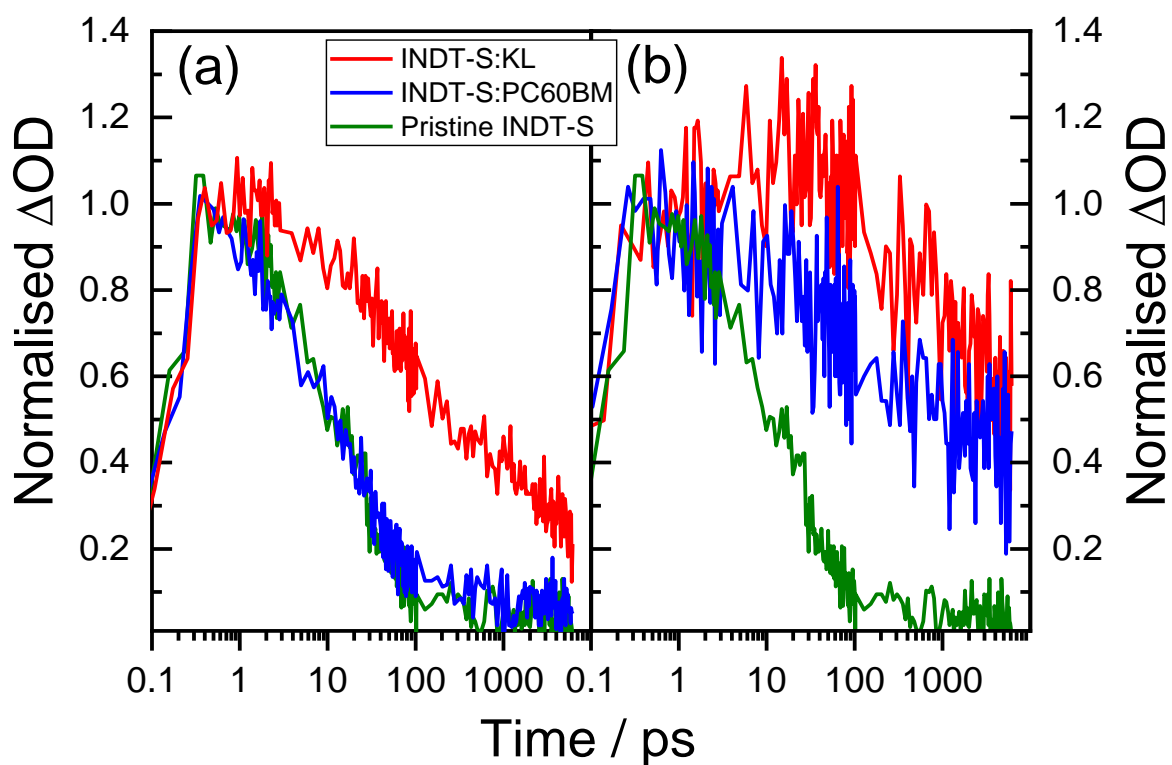


Figure 2: Picosecond TAS of INDTS:PCBM and INDTS:KL blend films probed at 1200 nm for two excitation wavelength a) 800 nm and b) 450 nm and a similar excitation laser pulse energy of 45nJ. Both are compared to the pristine INDTS-S kinetics measured using 800 nm excitation (also 1200 nm probe, 45 nJ). The excitation wavelengths were chosen to study the selective excitation of either the donor or the acceptor. The probe wavelength 1200 nm is found to properly describe the rate decay of the different excited species present in the different blends.

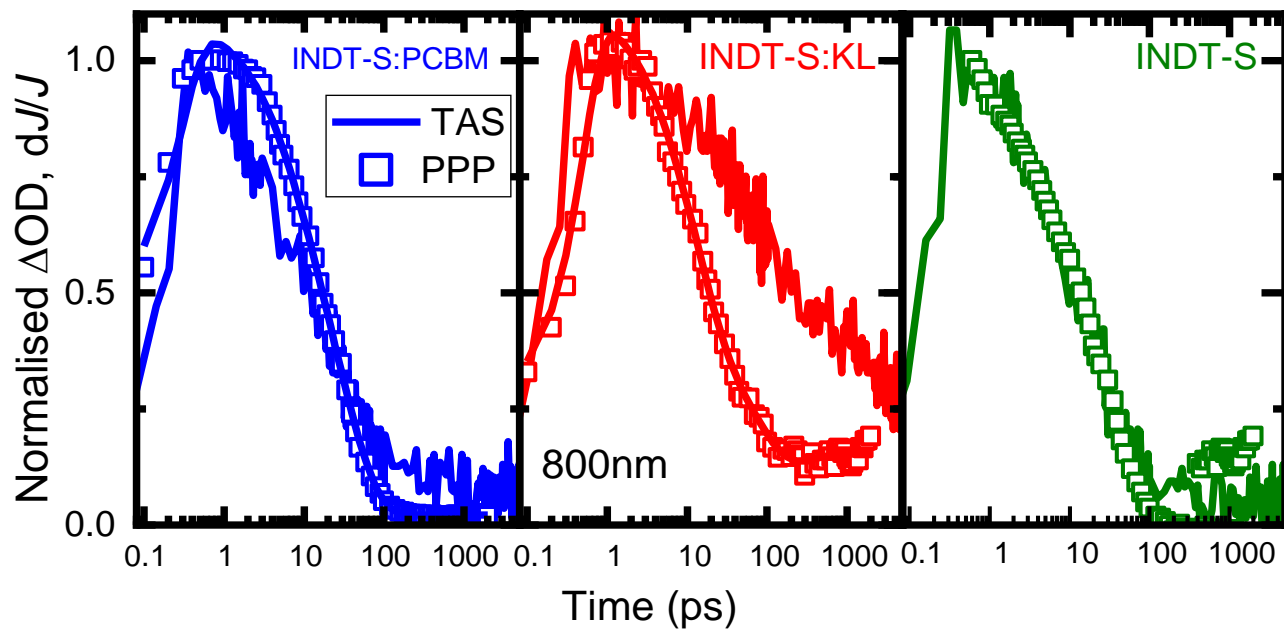


Figure 3: Kinetics of the ps-TAS of INDTS:PCBM and INDTS:KL blend films and pristine INDTS-S probed at 1200 nm, compared to the normalized PPP signal with an excitation at 800nm and a push laser wavelength of 2000nm.

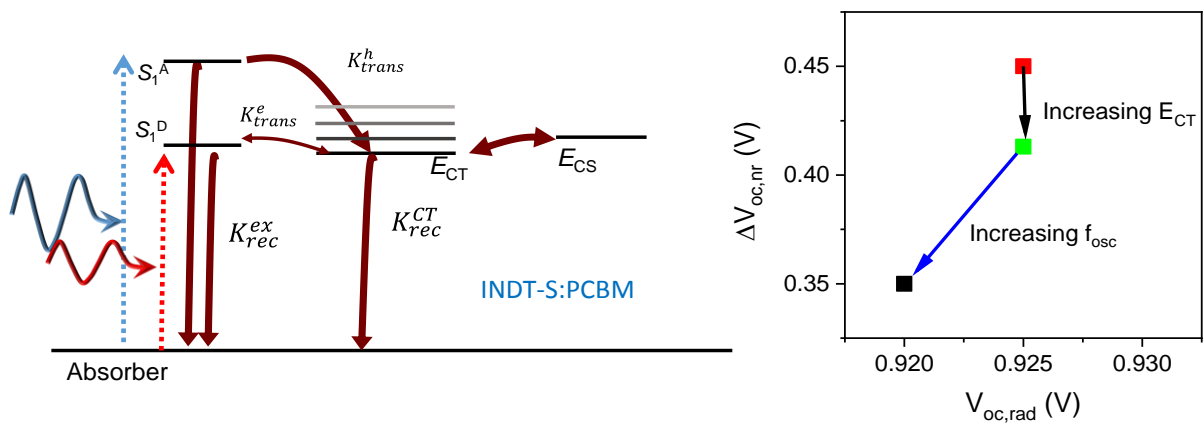


Figure 4 a) the kinetic model used to describe the evolution of the excited species, b) model results for the non-radiative losses.

Table 2 Rate parameters used to fit the ps-TAS spectra with the kinetic model. The rate for the exciton recombination ( $K_{rec}^{ex}$ ) was estimated by fitting the decay of the ps-TAS for the pristine IND-T-S films. The ps-TAS spectra of the blends at different excitation wavelength (450nm and 800nm) were fitted with the same rates apart from the rate of transfer from the exciton to the CT state that depend on whether the donor was photo-excited ( $K_{trans}^e$ ) or the acceptor was photo-excited ( $K_{trans}^h$ ).  $K_{rec}^{CT}$  the rate of decay to the ground state from CT state,  $K_{trans}^{CT,CS}$  the rate of transfer from the CT state to the Charge separated state,  $K_{trans}^{CS,CT}$  the rate of back-transfer from the Charge separated state to the CT state,  $K_{trans}^{CT,S1}$  the rate of back-transfer from the CT state to the exciton state. N.B : when fitting the decay of the KL:IND-T-S blend with the 450nm excitation wavelength the rates  $K_{rec}^{CT}$  and  $K_{trans}^{CT,CS}$  had to be changed, the values in brackets are the ones used to fit the 450nm excitation spectra).

Rate in ps <sup>-1</sup>	PCBM:IND-T-S	KL:IND-T-S
$K_{trans}^e$	$1.5 \pm 0.3 \cdot 10^{-2}$	$4 \pm 1 \cdot 10^{-1}$
$K_{trans}^h$	$3 \pm 1 \cdot 10^{-1}$	$10^0$
$K_{rec}^{ex}$	$7 \pm 0.3 \cdot 10^{-2}$	$7 \pm 0.3 \cdot 10^{-2}$
$K_{rec}^{CT}$	$8 \pm 1 \cdot 10^{-3}$	$4 \pm 1 \cdot 10^{-3} (3 \pm 1 \cdot 10^{-4})$
$K_{trans}^{CT,S1}$	$2 \pm 1 \cdot 10^{-3}$	$1 \pm 1 \cdot 10^{-3}$
$K_{trans}^{CT,CS}$	$1 \pm 0.4 \cdot 10^{-2}$	$2 \pm 1 \cdot 10^{-3} (7 \pm 1 \cdot 10^{-4})$
$K_{trans}^{CS,CT}$	$< 10^{-3}$	$< 10^{-4}$